

Numerical Investigation of Fuel Pulsatile Flow Through Wavy Channel

Ameer K. Salho¹, Hameed K. Hamzah², Ahmed M. Hassan³, Farooq H. Ali^{2*},
Qusay Rasheed Al-Amir^{2, 4}

¹Republic of Iraq Ministry of Electricity, Al-Qadisiyah, 58001, Iraq.

²Department of Mechanical Engineering University of Babylon-Babylon-Iraq. Hilla, 51001, Iraq.

³Department of Mechanical Engineering, University of Al-Qadisiyah, Al-Qadisiyah, 58001, Iraq.

⁴Air Conditioning and Refrigeration Techniques Engineering Department, Al-Mustaqbal University College, Babylon 51001, Iraq

Received 7 Oct 2023

Accepted 11 Feb 2024

Abstract

In this numerical study, the heat transfers of two types of fuels, namely kerosene and gasoline, were studied within a wavy channel with pulsed flow. The CFD module at COMSOL Multiphysics was used in this study. Several variables were used and applied to both types of fuel and compared between them. These variables included the values of Reynolds numbers between 200 to 800, as well as several values of Strouhal Numbers between 0 to 0.25. Different variable values were also used for the wavy channel, including the wave numbers (0, 2, 4, 6, 8, 10) as well as variable values of the wave amplitude (0, 0.1, 0.2, 0.3). Through this study, it was observed that as Strouhal Numbers increase, there is an increase in the Nusselt Number value. It was also observed that as the number of waves increases, there is an improvement in the heat transfer values. The numerical results showed that the values of heat transfer improved with an increase in the amplitude of the wave..

© 2024 Jordan Journal of Mechanical and Industrial Engineering. All rights reserved

Keywords: Kerosene, Fuel, wave channel, Pulsatile Flow, Microchannels.

1. Introduction

The heat transfer process is one of the most important problems facing researchers and engineers in all facilities and industrial engineering applications. Thermal improvement methods are many and varied due to the fact that the issue of heat transfer has become an inseparable problem in all machines that operate periodically. Therefore, the need has become necessary to find methods that help in the process of thermal improvement, including the use of heat exchangers with a larger cross-sectional area, as well as the use of small and micro-channels. Also, the pulsating flow within Wavy channel is one of the methods used in the thermal improvement process as presented by Zontul et al. [1].

Many researchers have studied the effect of pulsating flow on the heat transfer process. Mohammad Jafari et al. [2] presented a study on the effect of convective heat transfer on the pulsating flow within a corrugated channel. They studied the effect of changing the pulse frequency and oscillation amplitude on the process of heat transfer. They found that the process of heat transfer in the pulsating flow largely depends on the pulse velocity coefficients. The rate of heat transfer in a pulsating flow is highly dependent on the change of the Strouhal number. Nandi and Chattopadhyay [3] presented a study on the simultaneously developing unstable laminar flow and heat transfer within a corrugated Nano channel. They studied the effect of wave

amplitude as well as frequency on the heat transfer performance. They found that increasing amplitude and frequency leads to improving of the thermal performance. Akdag et al. [4] studied the water-based nanofluids (Al_2O_3) in a small corrugated channel under the influence of pulsating flow. The results of the research showed that the heat transfer process increases with the increase in the size of the nanoparticles and the increase in the amplitude of the pulse. Many studies enhanced the thermal properties of pulsating flow by adding the nano-particles to working fluids [5-10], and some studies used vortex generator in the flow passage [11-20]. Zhang et al. [21] studied the effect of pulsating flow on the heat transfer performance of the pseudo-plastic fluid flow in the heat sink in small channels. The heat transfer of the three functions in pulsating flow is better than in static flow. The study also proved that the sinusoidal function in the pulsating flow has a better thermal improvement rate than the other functions. This type of channel is used in many applications in particular, such as electronic devices cooling [22, 23]. Many studies focused on the shape of channel and many of them used different shapes of obstacles inside the channel V-shaped, twisted spirals, grooves ribs, dimples, etc. [24-29] to improve the thermal performance of channel. The channel shape or flow past around the obstacles, and the location of obstacles have major impact on the thermal and dynamic performance of channel as investigated by [30, 31]. The heat transfer parameter of pulsated flow in wave channel was studied by [32-34]. Other studies focused on the

* Corresponding author e-mail: eng.farooq.hassan@uobabylon.edu.iq.

hydrodynamics and heat transfer such as [35-39]. The use of nanofluids with pulsed flow was studied by [40-48] where wave and corrugated channel were used during these studies. A number of numerical and experimental studies investigated non-Newtonian fluid's heat transfer inside the wave channel and under the pulsate flow [49-51]. The wave channel has been used widely in application of heat exchangers which are able to efficiently produce secondary flow and vortexes in ducts that greatly improve the heat transfer performance [52-56]. Multiple methods have been used to improve heat transfer through channels, and one of these methods is the use of porous media, as in [57-60]. These types of channels are often used in heat exchanger applications [61]

It can be noticed that most of the previous studies focus on the type of channel used as well as the liquid used, which is water. In the current study, the effect of pulsating flow on heat transfer using two types of fuel was employed, as well as a change in the structure of the wavy channel used. Enhancing heat transfer performance is critical for improving energy efficiency in systems like fuel processing, chemical reactors, and electronics cooling. Prior studies show that pulsating flows and surface modifications can augment heat transfer, but analyses of pulsation in non-straight geometries are limited. This study aims to address the knowledge gap by numerically investigating pulsating flow in wavy channels across a range of parameters. The results will provide new insights into designing optimized heat exchangers and reactors by manipulating channel geometries and pulsation conditions. This investigation fills a critical need for comprehensively understanding pulsation in wavy geometries to advance heat transfer capabilities in thermal engineering applications.

2. Numerical model

2.1. Physical Domain

In this study, a two-dimensional wave channel has been used studying the pulsating flow through it. This channel has a known dimension where (H) represents the height of the channel and (20H) represents the length of the channel as shown in figure (1). The channel consists of three regions, the first region represents the entrance region, which is flat, and its length is (3H), and the second region is the region of the wavy channel, which is wavy with sinusoidal function as in the following equation [62]:

$$y = \alpha \sin\left(2\pi\beta \frac{x - x_i}{x_o - x_i}\right) \quad (1)$$

Where β is wavy number, α wavy amplitude of channel, sub-scripts i and o represented the inlet and outlet section, respectively. The third part of the channel is a flat and its length 5H.

2.2. Governing equations and assumptions

The numerical simulations were conducted under specific conditions, including: a single phase, two-dimensional, laminar, and incompressible flow of fluid. The thermophysical properties of the fluid were assumed to be constant, and the effects of gravity and radiation heat transfer were disregarded. The flow was transient and pulsatile in nature, but fully developed. Additionally, the fluids used in the simulations were assumed to be Newtonian, and both kerosene and gasoline were studied.

The equations that govern the flow and heat transfer in the system are the continuity equation, Navier-Stokes equation, and energy equation. The two-dimensional equations for constant thermophysical properties are written as follows:

Continuity equation

$$\frac{\partial \rho}{\partial t} + \frac{\partial(\rho u)}{\partial x} + \frac{\partial(\rho v)}{\partial y} = 0 \quad (2)$$

Navier-stoke equation

In x-direction:

$$\rho \left(\frac{\partial u}{\partial t} + u \frac{\partial u}{\partial x} + v \frac{\partial u}{\partial y} \right) = -\frac{\partial p}{\partial x} + \mu \left(\frac{\partial^2 u}{\partial x^2} + \frac{\partial^2 u}{\partial y^2} \right) \quad (3)$$

In y-direction:

$$\rho \left(\frac{\partial v}{\partial t} + u \frac{\partial v}{\partial x} + v \frac{\partial v}{\partial y} \right) = -\frac{\partial p}{\partial y} + \mu \left(\frac{\partial^2 v}{\partial x^2} + \frac{\partial^2 v}{\partial y^2} \right) \quad (4)$$

Energy equation:

$$\rho c_p \left(\frac{\partial T}{\partial t} + u \frac{\partial T}{\partial x} + v \frac{\partial T}{\partial y} \right) = k \left(\frac{\partial^2 T}{\partial x^2} + \frac{\partial^2 T}{\partial y^2} \right) \quad (5)$$

Since the current study is a numerical study only, there is no experimental work that has been studied. Therefore, it is better to convert the solution to dimensionless solutions, this will provide many advantages such as:

1. Ease of knowing when to apply familiar mathematical relationships.
2. It lowers the number of times we may need to solve the problem numerically.
3. It offers us insight into what may be minor characteristics that may be overlooked or dealt with roughly.

Therefore, the non-dimensional variables that will be used as follows [56]:

$$(U, V) = \frac{(u, v)}{u_o}, \quad (X, Y) = \frac{(x, y)}{H}, \quad P = \frac{p}{\rho u_o^2},$$

$$\theta = \frac{T - T_i}{T_s - T_i}, \quad \tau = \frac{t u_o}{H}, \quad Re = \frac{\rho u_o H}{\mu}, \quad Pr = \frac{C_p \mu}{k}$$

Where u_o is the main flow velocity, sub-scripts i and s represented the inlet section and channel heated surface, respectively.

non-dimensional form of governing equations becomes:

Continuity equation:

$$\frac{\partial U}{\partial \tau} + \frac{\partial V}{\partial Y} = 0 \quad (6)$$

Momentum equation:

In x-direction

$$\frac{\partial U}{\partial \tau} + U \frac{\partial U}{\partial X} + V \frac{\partial U}{\partial Y} = -\frac{\partial P}{\partial X} + \frac{1}{Re} \left(\frac{\partial^2 U}{\partial X^2} + \frac{\partial^2 U}{\partial Y^2} \right) \quad (7)$$

In y-direction

$$\frac{\partial V}{\partial \tau} + U \frac{\partial V}{\partial X} + V \frac{\partial V}{\partial Y} = -\frac{\partial P}{\partial Y} + \frac{1}{Re} \left(\frac{\partial^2 V}{\partial X^2} + \frac{\partial^2 V}{\partial Y^2} \right) \quad (8)$$

Energy equation:

$$\frac{\partial \theta}{\partial \tau} + U \frac{\partial \theta}{\partial X} + V \frac{\partial \theta}{\partial Y} = \frac{1}{Re Pr} \left(\frac{\partial^2 \theta}{\partial X^2} + \frac{\partial^2 \theta}{\partial Y^2} \right) \quad (9)$$

The general equation of Nusselt number can be calculated from [64]

Local:

$$Nu = \left(\frac{-H}{T_{wall} - T_{in}} \right) \left(\left(\frac{\partial T}{\partial n} \right)_{\text{Bottom Wall}} + \left(\frac{\partial T}{\partial n} \right)_{\text{Top Wall}} \right) \quad (10)$$

Where (n) represents the normal direction to the surface. Space averaged:

$$Nu_{\bar{x}} = \frac{1}{(x_o - x_i)} \int_{x_i}^{x_o} Nu ds \quad (11)$$

Space and period averaged:

$$Nu_{\bar{\tau}} = \frac{1}{\tau} \int_0^{2\pi} Nu_{\bar{x}} d\tau \quad (12)$$

Where p is dimensionless time parameter.

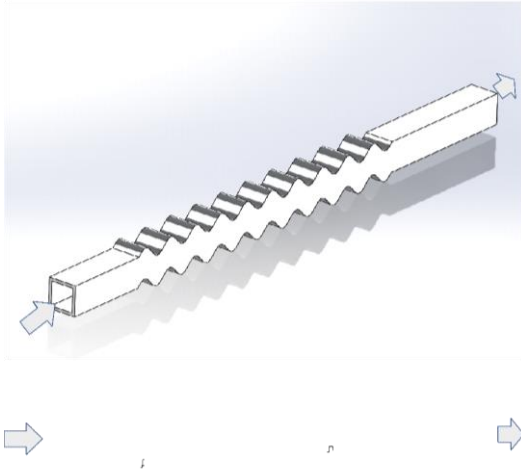


Figure 1. Schematic view of channel.

2.3. Boundary condition

The boundary conditions which used the current study are shown in figure (2). The wave wall was under constant temperature and other walls were insulated. The pulsatile inlet velocity can be represented in figure (3). The momentum and thermal boundary can be represented as follows:

Momentum boundary conditions

At channel inlet line A-B

$$U(Y, \tau) = \frac{3}{2} u_0 (1 - (Y - 1)^2) [1 + \alpha \sin(2\pi St \tau)] \quad (13)$$

The Strouhal number, denoted by (St), is a non-dimensional frequency parameter that is defined as[4]:

$$St = \frac{fH}{u_0} \quad (14)$$

Where f is the frequency of vortex shedding

At lines A-C, B-D, C-E, D-F, E-G, and F-H, the boundary condition was no-slip boundary condition: $U = V = 0$.

At the outlet line G-H ($P_o = 0$)

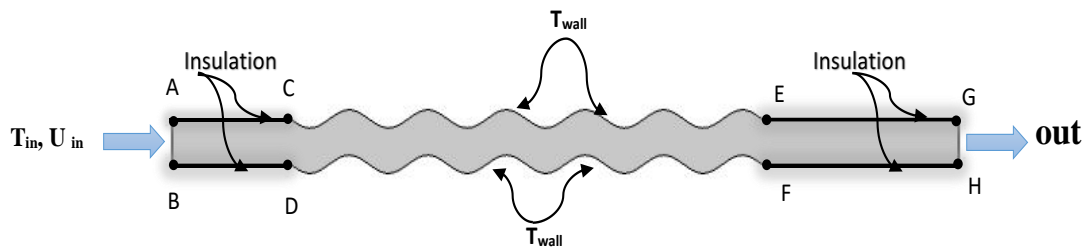


Figure 2. Boundaries of domain.

Energy boundary conditions

At inlet (line A-B) $\theta = 0$

At insulated wall (A-C, B-D, E-G, F-H) $\frac{\partial T}{\partial y} = 0$

At heated wall (C-E, D-F) $\theta = 1$

The percentage of improvement in Nusselt number value can be found by using the following relationship:

$$Enhancement = \frac{Nu_{wave} - Nu_0}{Nu_0} \quad (15)$$

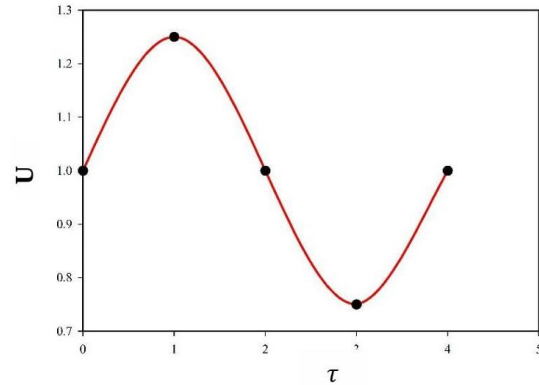


Figure 3. Pulsatile inlet velocity.

2.4. Numerical procedures

To solve the problem at hand, the CFD code COMSOL 5.5 was utilized. A finite element method on a collocated grid was employed to discretize the governing equations. The SIMPLE algorithm was used to solve these equations, with convection and diffusion terms being discretized using second order upwind schemes. Under-relaxation was performed on the velocities, pressure, and temperature to ensure convergence of the numerical solution.

The convergence criterion for both energy and flow equations was set to 10^{-6} . The mesh was finer near the walls to accurately resolve the high gradients in the thermal and hydrodynamic boundary layer, as depicted in figure (4). Additionally, grid independence was assessed to obtain an optimal grid distribution that provides accurate results within minimal computational time. Five grid resolutions were used to accomplish this, as shown in Table (1). The time average Nusselt number at ($\beta=6$, $\alpha=0.2$, $Re=800$, $Pr=31.4$, and $St=0.25$). For the grid with (39066), it gives a lower value of error (4.7%). The figure shows the target $y+$ value (e.g. $y+ < 1$) for accurate wall function resolution at $Re=800$ and the increased mesh density near walls to capture boundary layer gradients. As explained in the figure, the mesh independence study shows convergence of velocity/temperature profiles and Nusselt number at $Re=800$.

2.5. Validations

To ensure that the numerical findings of current work are accurate, which is achieved using COMSOL Multiphysics software, the outcomes of the present code were compared with the results of other researches. The numerical solution was validated with the published work of Zontul et al. [1], where this study included laminar pulsating flow of water ($Pr=6.93$) in wavy channel. The comparison of the solution program is used in this study with Zontul et al. [1] results as illustrated in Figures (5) and (6).

Table 1. Grid independent test

Grid	Maximum face size	Number of elements	Nusselt Number
G1	0.5	4142	56.4332
G2	0.4	4220	58.3478
G3	0.2	7276	66.4986
G4	0.08	39066	89.6127
G5	0.06	67106	116.8322

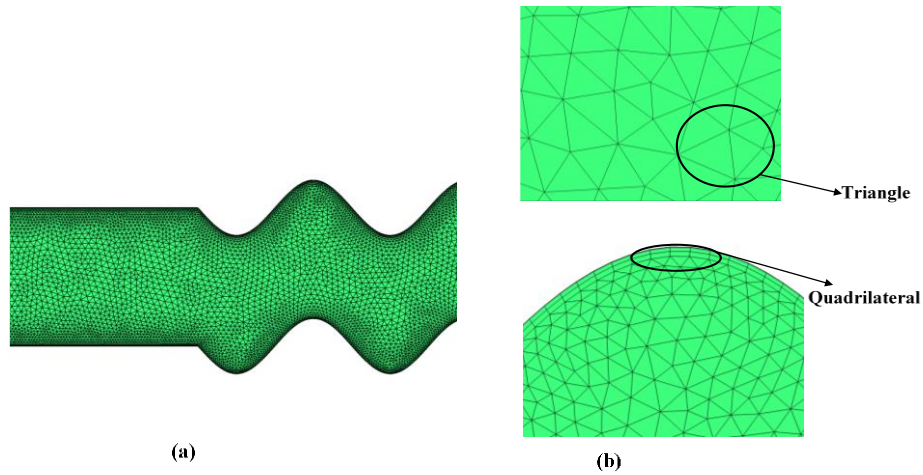


Figure 1. Grid distribution.

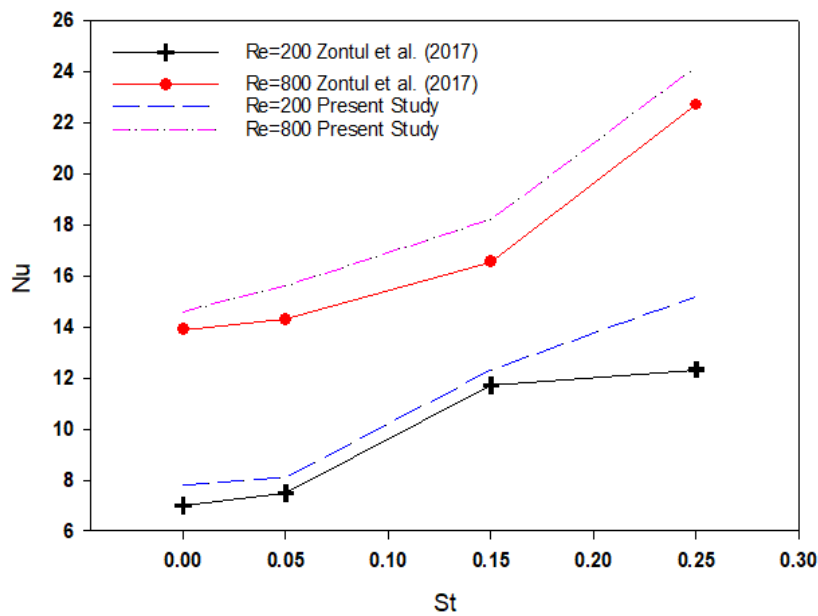


Figure 2. Comparison between the current study software results and the study of Zontul et al. [1], Time-averaged Nusselt number variation with Strouhal numbers.

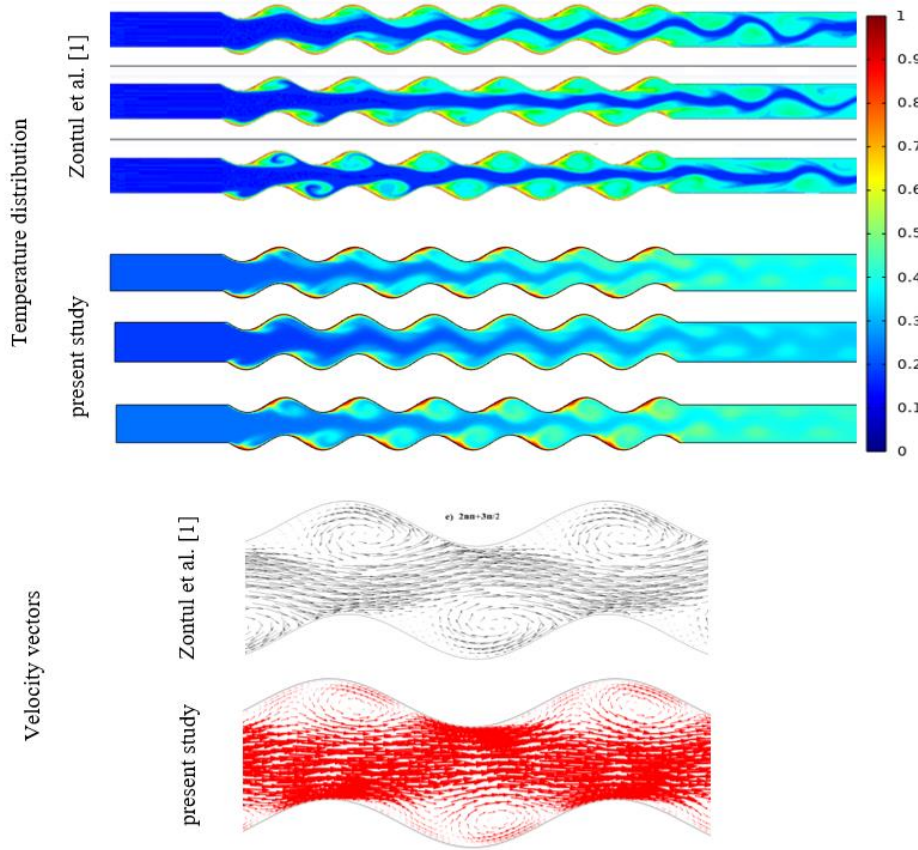


Figure 3. Temperature distribution and velocity vectors inside the channel by Zontul et al. [1] and present study at $St = 0.15$, $Re=400$, $\beta=3$, $Pr=6.93$ and $\alpha=0.2$.

2.6. Working Fluid

In this study, the focus was on the use of fuel as working fluid, and this reflects the many applications in which the wavy channel can be used to transport through them. Where kerosene and gasoline were used as a model for the study. The thermos-physical properties of the two working fluids are represented in **table (2)**.

Table 2. Properties of working fluid.

	kerosene	gasoline
Property	Value	Value
Prandtl number	31.4	8.19
Thermal conductivity ($W/m K$)	0.145	0.15
Kinematic Viscosity(cSt)	2.71	0.553
Specific heat ($kJ/(kg K)$)	2.01	2.22
Density(kg/m^3)	840	780

3. Results

Three important cases were used and compared with the effect of heat transfer. These three cases were used with four types of Reynolds number (Re) (200, 400, 600, 800), where THE first one includes the extent of the effect of changing Strouhal number (St) on heat transfer and flow, where three types of Strouhal number (St) were used (0, 0.05, 0.15, 0.25) as well as six types of wavy number (β) were also used (0, 2, 4, 6, 8, 10) observing the extent of the effect of changing

the number of wavy number at each Reynolds number and its impact on the improvement of heat transfer and pulsating flow. Finally, three types of wavy amplitude (α) were used, namely (0, 0.1, 0.2 , 0.3), and all the variables were used for two types of fuel.

Figure (7) explains the distribution of the Nusselt number along the smooth channel. It can be seen that Nusselt number is stable along the channel at the value of (12.536) and then it rises in the exit area. The stability of Nusselt number is due to the stability of the temperature difference between the wall and the fluid entering the channel. Nusselt number can be seen changing over time as it fluctuates due to the change of pulsed flow. In the case of the wavy channel, the Nusselt number rises at the wavy areas, as can be seen in the **figure (8)**. Where Nusselt number fluctuates between 4.9 to 50. This is due to the corrugation areas forming narrowing areas between the upper and lower walls, and thus the heat transfer coefficient increases. **Figure (9)** shows the local Nusselt number distribution at wavy channel. It can be seen that the fluctuation of the curve increases when the wavy number increases, because the wavy number leads to an increase in the number of peaks through the channel, which forms a narrow path that passes through the fluid, and thus its velocity increases, which increases the heat transfer coefficient and the Nusselt number.

Figure (10) shows the relation between time-averaged Nusselt number and Reynolds number. The relationship between $Nu_{a,t}$ and Re at different Strouhal numbers may be influenced by a variety of factors, including the geometry of

the channel, the amplitude and frequency of the waves, and the properties of the fluid. As the Reynolds number increases, the flow becomes more turbulent, which can lead to an increase in the time-averaged convective heat transfer coefficient and, consequently, an increase in the time-averaged Nusselt number. However, the effect of Reynolds number on $Nu_{\bar{t}}$ may depend on the specific flow conditions and the Strouhal number. It can be noticed that Nusselt number reaches its highest value at $Re=800$ as well as at the highest value of $Nu_{\bar{t}}$ are $Nu_{\bar{t}}=102.4$ for $St=0$ and $Nu_{\bar{t}}=116.05$ for $St=0.15$.

At low Strouhal numbers, the waves in the channel may induce more mixing in the fluid, which can lead to an increase in the time-averaged convective heat transfer coefficient and, consequently, an increase in the time-averaged Nusselt number as explained in **figure (11)**. At high Strouhal numbers, the waves may create a more laminar flow regime, which can lead to a decrease in the time-averaged convective heat transfer coefficient and a decrease in the time-averaged Nusselt number. The relationship between the variation of the Nusselt number with time and the Strouhal number can provide valuable insights into the temporal heat transfer characteristics of pulsatile flow through a wavy channel.

Figure (12) shows the effect of wavy number of the time-averaged Nusselt number. At low Reynolds numbers, the flow in the channel may be dominated by viscous effects, which can lead to less heat transfer enhancement due to the waves. As the Reynolds number increases, the flow becomes more turbulent, which can lead to an increase in the time-averaged convective heat transfer coefficient and, consequently, an increase in the time-averaged Nusselt number. The relationship between $Nu_{\bar{t}}$ and β may depend on the specific flow conditions and the Reynolds number. In general, as the wavy number increases, the degree of wave-induced flow distortion increases, which can lead to more heat transfer enhancement due to the waves. However, at very high wavy numbers, the wave-induced flow distortion may become so severe that it leads to a decrease in the time-averaged convective heat transfer coefficient and a decrease in the time-averaged Nusselt number.

Figure (13) depicts the effect of wavy amplitude on the time-averaged Nusselt number. The wavy amplitude (α) is defined as the maximum deviation of the channel wall from a straight line. It is a measure of the degree of wave-induced flow distortion in the channel. In general, as the wavy amplitude increases, the degree of wave-induced flow distortion increases, which can lead to more heat transfer enhancement due to the waves.

Figure (14) shows the relation between Re and the time-averaged Nusselt number for two types of fuel. The time-averaged Nusselt number is directly proportional to the Reynolds number. This means that as the Reynolds number increases, the time-averaged convective heat transfer coefficient increases, leading to an increase in $Nu_{\bar{t}}$. This relationship is based on the fact that higher Reynolds numbers are associated with increased turbulence and mixing in the flow, which enhances the convective heat transfer. The exact nature of the relationship between $Nu_{\bar{t}}$ and Re for gasoline and kerosene may depend on the specific fluid properties of these fuels, including their thermal conductivity, specific heat capacity, and viscosity. For example, kerosene is typically more viscous than

gasoline, which can affect the degree of turbulence and mixing in the flow, and consequently the convective heat transfer coefficient and $Nu_{\bar{t}}$. Kerosene has higher thermal conductivity and lower volatility compared to gasoline. The higher thermal conductivity of kerosene may lead to higher Nusselt numbers compared to gasoline under certain flow conditions. Additionally, the lower volatility of kerosene may make it more suitable for high-temperature applications where evaporation of the fuel may not be desirable. The wavy number (β) is one of the important parameters that can affect the convective heat transfer and consequently the Nusselt number ($Nu_{\bar{t}}$) in wavy channels. The effect of the wavy number on the Nu for kerosene and gasoline flow in wavy channels can depend on several factors, including the channel geometry, the flow conditions, and the fluid properties of the fuels as explained in **figure (15)**. Increasing the wavy number can enhance the heat transfer in wavy channels. This is because the wavy walls create additional secondary flows and enhance the turbulence in the flow, which can increase the convective heat transfer. Kerosene has a higher thermal conductivity than gasoline, then increasing the wavy number may result in a greater enhancement of heat transfer for kerosene flow compared to gasoline flow.

Figure (16) depicts the effect of Strouhal number (St) on the streamlines and isotherm contours. St is a dimensionless parameter that represents the unsteady behavior of a fluid flow. It is defined as the product of the vortex shedding frequency and the characteristic length scale of the flow divided by the fluid velocity. The effect of the Strouhal number on the streamlines and isotherm contours in a flow field can depend on several factors, including the geometry of the flow, the flow conditions, and the fluid properties. In general, for low Strouhal numbers, the flow is steady, and the streamlines and isotherm contours are fixed. As the Strouhal number increases, the flow becomes more unsteady, and the streamlines and isotherm contours begin to oscillate. This oscillation can manifest itself in several ways, including vortex shedding, which is the formation of alternating vortices in the flow, and the periodic variation of the boundary layer thickness.

Figure (17) shows the effect of wavy number on the streamlines and isotherm contours. The presence of waves in a channel creates additional secondary flows and can enhance the mixing in the flow field. This can lead to changes in the streamlines and isotherm contours. As the wavy number increases, the amplitude of the waves increases, and the wavelength of the waves decreases. This can lead to a more complex flow field with more pronounced secondary flows, which can cause more significant changes in the streamlines and isotherm contours. In the case of a wavy channel with low wavy number, the flow may resemble that of a straight channel, and the streamlines and isotherm contours may follow a similar pattern. As the wavy number increases, the flow becomes more complex, and the streamlines and isotherm contours may begin to deviate from their straight path, indicating more significant mixing in the flow. In a wavy channel with a small amplitude of waves, the effect of the wavy number on the streamlines and isotherm contours may be small. In contrast, in a wavy channel with a large amplitude of waves, the effect of the wavy number on the streamlines and isotherm contours may be more significant.

Table (3) explains the percentages of improvement in value of Nusselt number when increasing the wavy number. As the wavy number increases, the amplitude of the waves increases, and the wavelength of the waves decreases. This can lead to a more complex flow field with more pronounced secondary flows, which can cause more significant changes in the value of Nusselt number. The percentage of improvement in the value of Nusselt number when increasing the wavy number can vary depending on the specific wavy channel geometry and flow conditions. The increase in the wavy number leads to an increase in the surface area of heat transfer. It is noted that the percentage of improvement was 1.439 at $Re=200$, and wavy number=10, while it reached highest value at $Re=800$, and

wavy number=8, where the improvement in $Nu_{\bar{t}}$ equal to 1.923.

The percentage of improvement in the value of Nusselt number when changing the amplitude of the waves in a wavy channel can depend on several factors, including the wavy number, the wavelength of the waves, and the flow conditions. In general, increasing the amplitude of the waves in a wavy channel can lead to an improvement in the heat transfer coefficient and an increase in the value of Nusselt number as shown in **table (4)**. However, it is important to note that the percentage of improvement in the value of Nusselt number may not be linear with changes in the amplitude of the waves. This is because the effect of the amplitude on the flow field can depend on the specific wavy channel geometry and flow conditions.

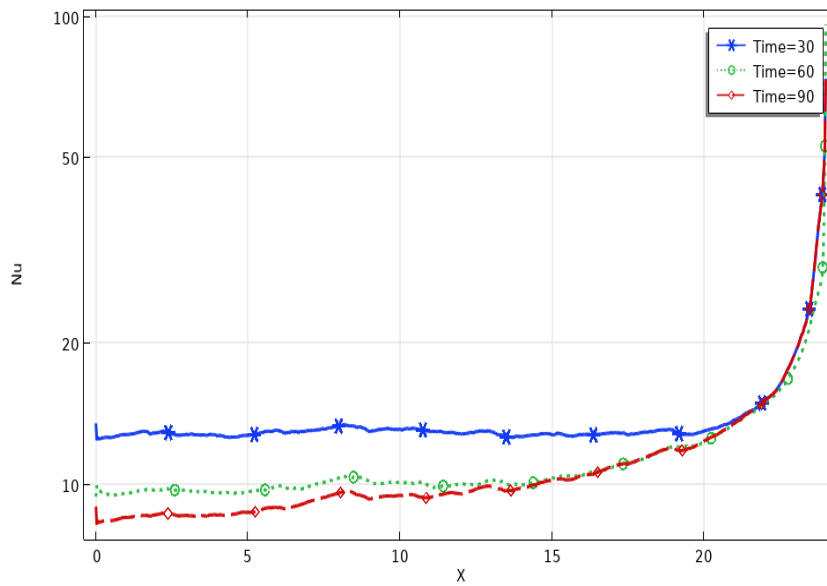


Figure 4. Local Nusselt number along the wall channel with $St = 0.15$, $Re=400$, $\beta=0$, $Pr=31.4$ and $\alpha= 0.2$ at different time.

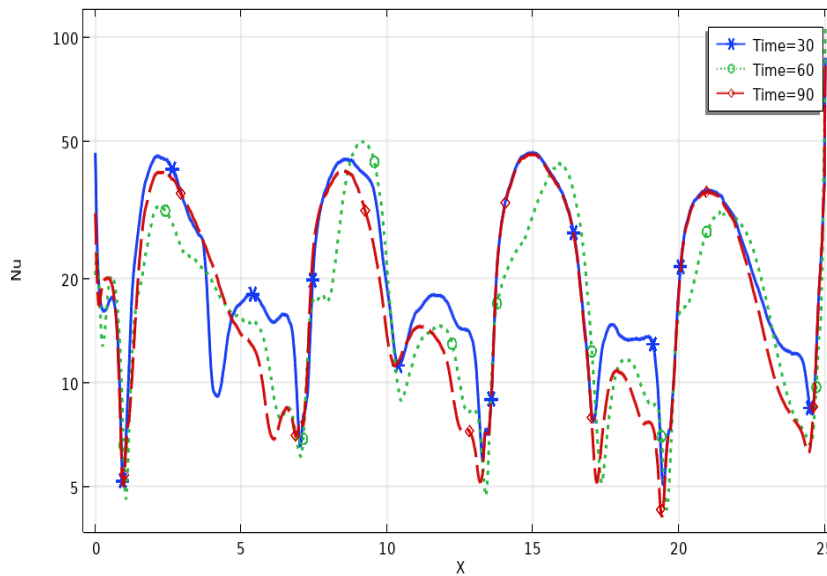


Figure 5. Local Nusselt number along the wall channel with $St = 0.15$, $Re=400$, $\beta=2$, $Pr=31.4$ and $\alpha= 0.2$ at different times.

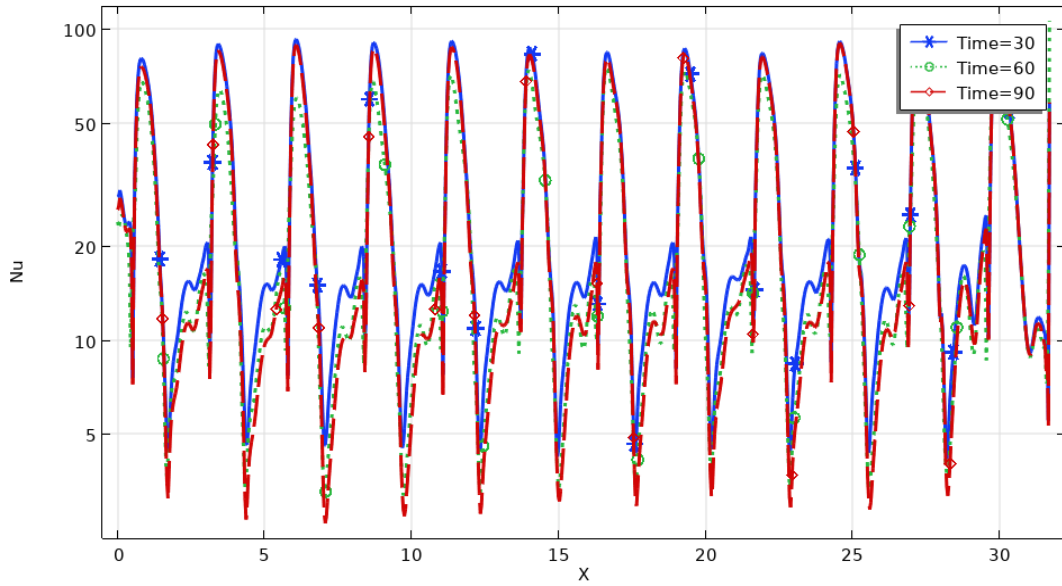


Figure 6. Local Nusselt number along the wall channel with $St = 0.15$, $Re=400$, $\beta=6$, $Pr=31.4$ and $\alpha=0.2$ at different time.

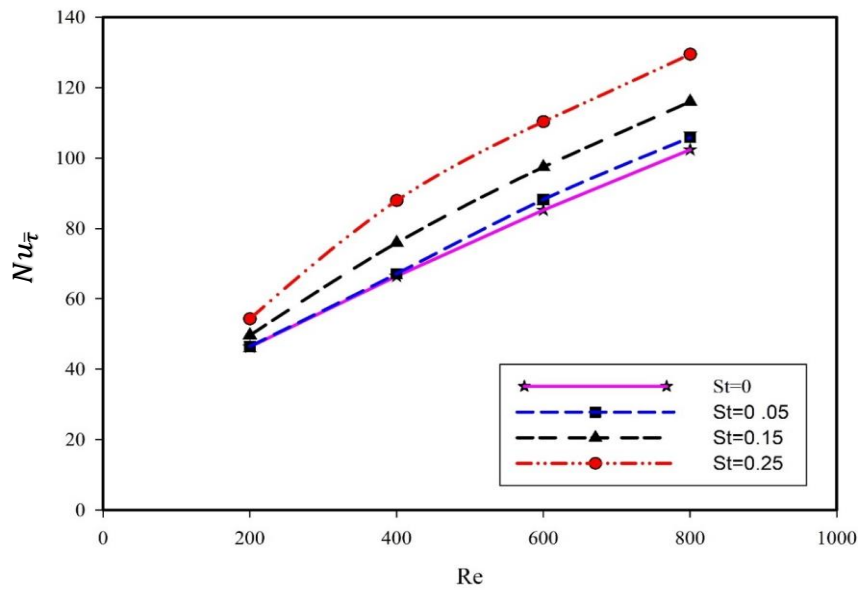


Figure 7. The relation between Time-averaged Nusselt number (Nu_{τ}) with Reynolds numbers (Re). (at $\beta=6$, $Pr=31.4$ and $\alpha=0.2$)

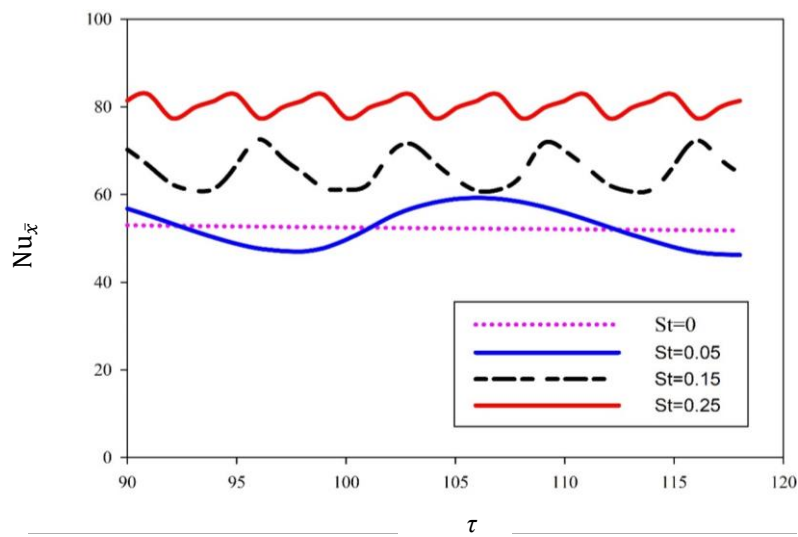


Figure 8. Variation of the Nusselt number (Nu_{τ}) with time for different Strouhal numbers (St) (at $Re=400$, $\beta=6$, $Pr=31.4$ and $\alpha=0.2$)

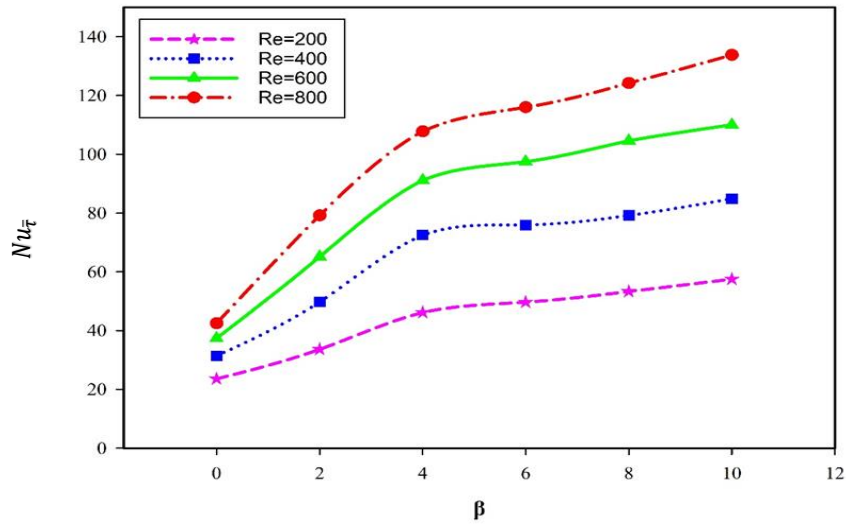


Figure 9. The relation between Time-averaged Nusselt number (Nu_T) with wavy number (β) at different Reynolds numbers (Re). (at, $St=0.15$, $Pr=31.4$ and $\alpha=0.2$)

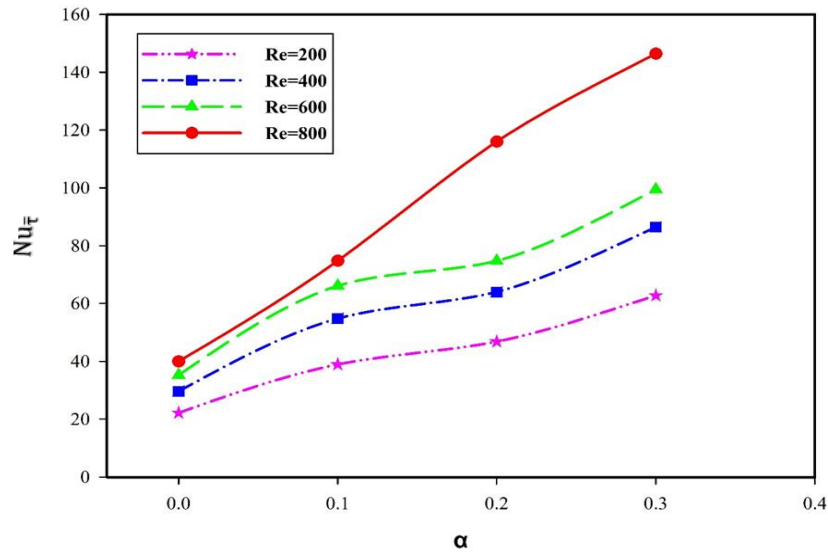


Figure 10. The relation between Time-averaged Nusselt number (Nu_T) with wavy amplitude (α) at different Reynolds numbers (Re). (at $St=0.15$, $\beta=6$, and $Pr=31.4$)

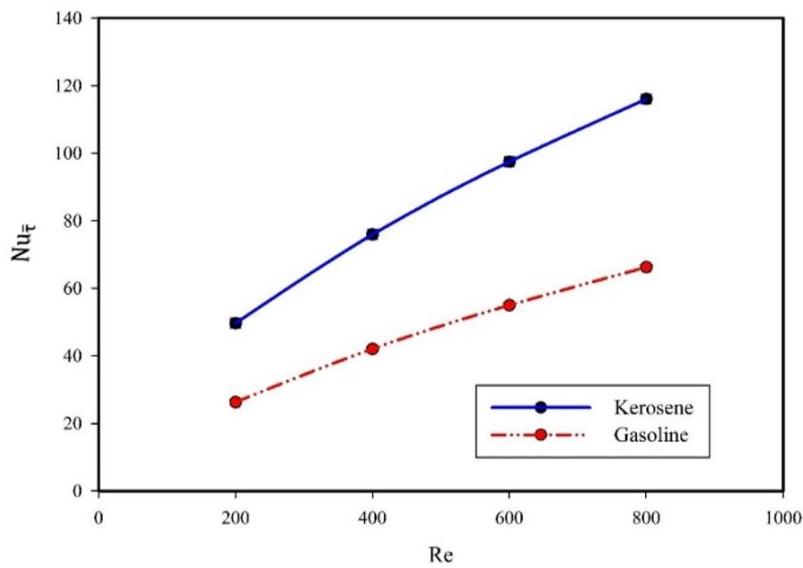


Figure 11. Relation between time-averaged Nusselt number (Nu_T) with Reynolds numbers (Re) for two types of fuel . (at $St=0.15$, $\beta=6$, and $\alpha=0.2$)

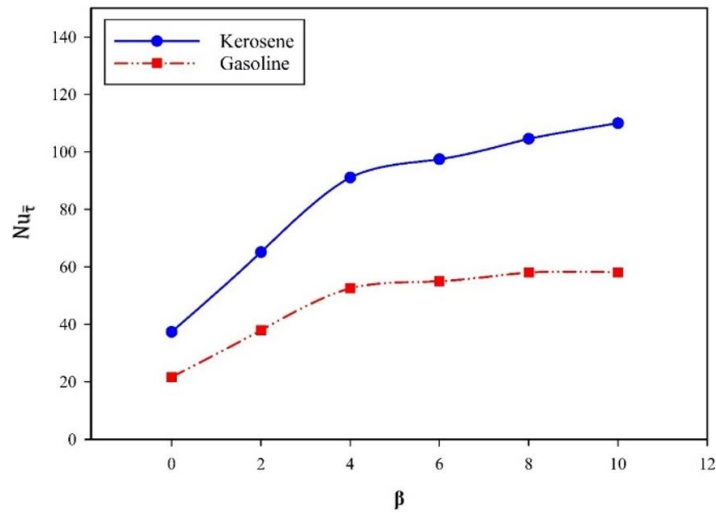


Figure 12. Relation between time-averaged Nusselt number (Nu_f) with wavy number (β) for two types of fuel. (at $St=0.15$, $Re=400$, and $\alpha=0.2$)

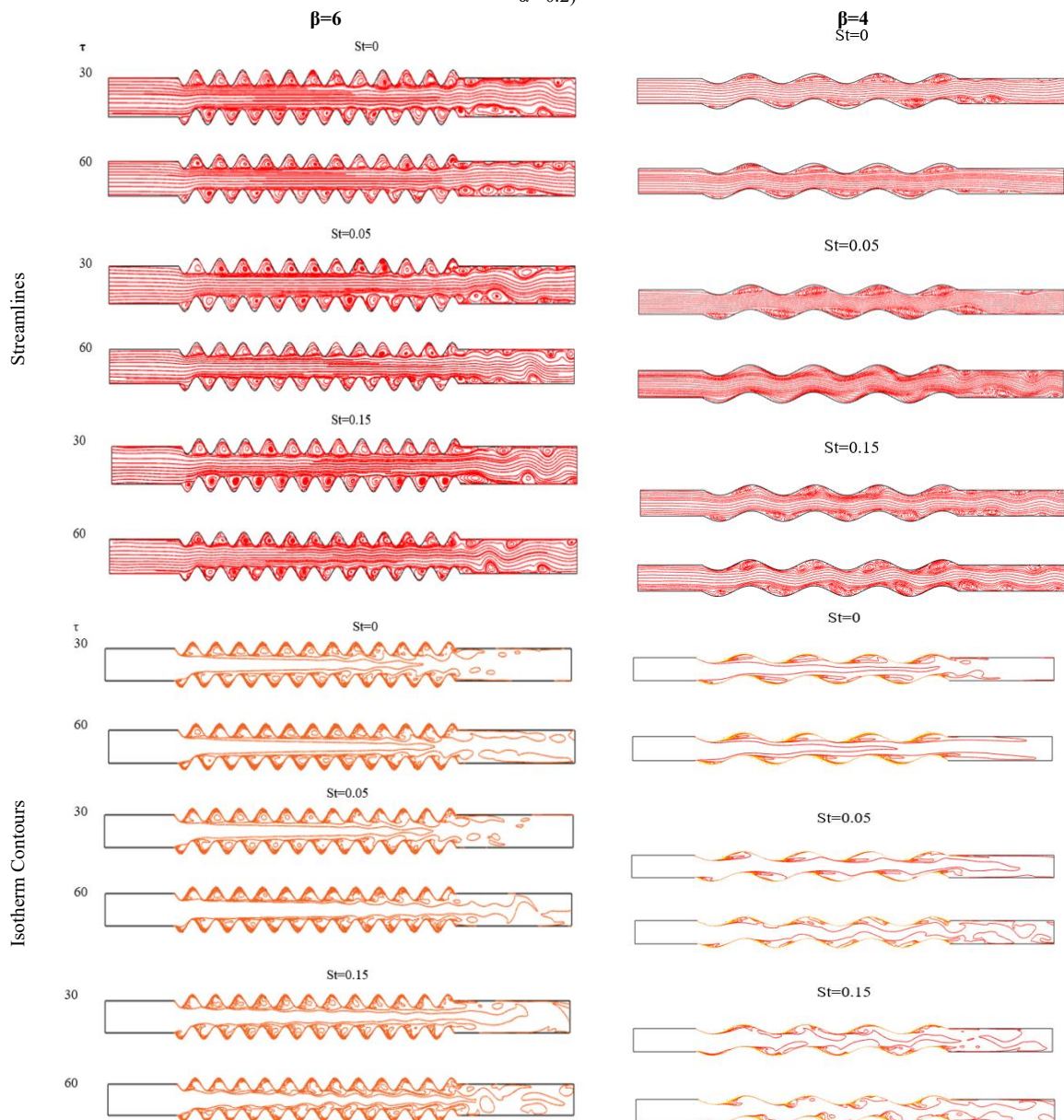


Figure 13. Effect of St number on the streamlines and isotherm contours for two value of wavy number at $Re=400$ and $\alpha=0.2$.

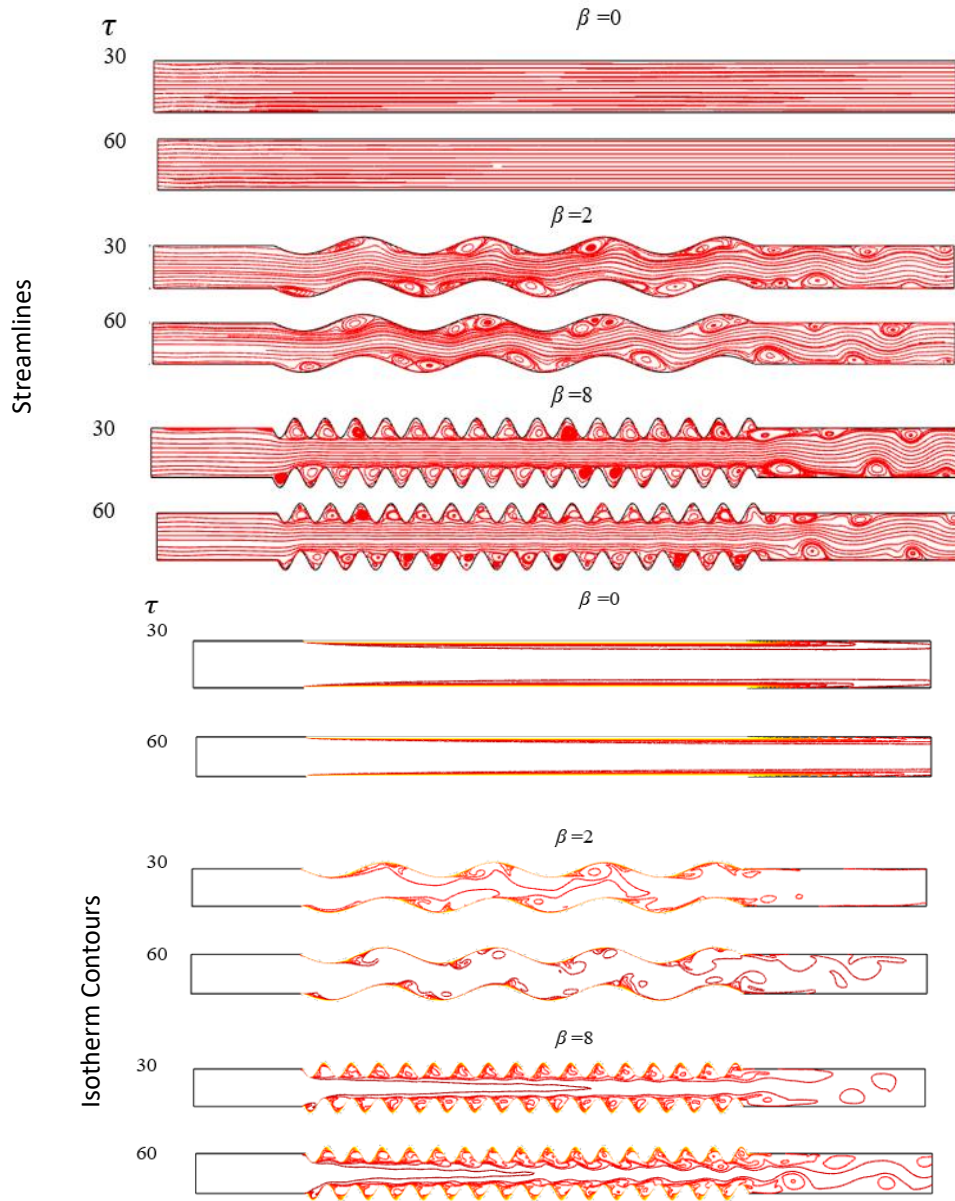


Figure 14. Effect of wavy number on the streamlines and isotherm contours.

Table 3. The percentage of improvement in the value of the Nusselt number when changing wave number at $\alpha = 0.2$

Re	Time-averaged Nusselt number					
	$\beta=0$	$\beta=2$	Enhancement	$\beta=4$	Enhancement	
200	23.56	33.61	0.426	46.14	0.957	
400	31.38	49.73	0.585	72.44	1.308	
600	37.36	65.11	0.742	91.13	1.438	
800	42.50	79.22	0.863	107.826	1.536	
Re	Time-averaged Nusselt number					
	$\beta=6$	Enhancement	$\beta=8$	Enhancement	$\beta=10$	Enhancement
200	49.66	1.106	53.31	1.262	57.49	1.439
400	75.93	1.419	79.22	1.524	84.91	1.706
600	97.48	1.608	104.60	1.799	110.04	1.944
800	116.05	1.730	124.263	1.923	133.798	2.147

Table 4. The percentage of improvement in the value of the Nusselt number when changing amplitude at $\beta=6$

Re	Time-averaged Nusselt number						
	$\alpha=0$	$\alpha=0.1$	Enhancement	$\alpha=0.2$	Enhancement	$\alpha=0.3$	Enhancement
200	22.16	38.91	0.756	46.78	1.111	62.744	1.831
400	29.59	54.80	0.851	63.96	1.161	86.392	1.919
600	35.24	66.10	0.875	74.70	1.119	99.451	1.821
800	39.97	74.77	0.870	116.05	1.902	146.45	2.663

4. Conclusions

Through this numerical study that was carried out on a wavy channel with a sinusoidal function and a pulsed flow, the dimensions of the channel were changed, which included the change in the number of waves as well as the wave height. It also studied several values of Reynolds number and Strouhal number, which shows the effect of pulsed flow of two types of fuels, kerosene and gasoline. Therefore, through this study, the following points can be concluded:

1. The results demonstrate that increasing the Reynolds number (Re), Strouhal number (St), wave amplitude (α), and wavy channel number (β) led to increases in the Nusselt number (Nu) for both kerosene and gasoline fuels.
2. Comparing the two fuels, gasoline has a higher value of Nu than kerosene under the same flow conditions.
3. The streamlines and isotherm contours are affected by both the Strouhal number and the wavy number, with higher values of St and β leading to more complex flow patterns.
4. Increasing the wavy number leads to a percentage increase in the value of Nu, but this percentage improvement may not be linear with changes in β .
5. Increasing the number of waves leads to an increase in the value of the Nusselt number. Compared to the flat channel, the percentage of improvement with the value of the Nusselt number reached 1.439 at the value of Reynolds number 200, while it reached 2.147 at the Reynolds number 800, and 10 wave number. Therefore, an increase in the Reynolds number leads to an increase in the improvement in heat transfer.
6. Through the numerical analysis, it was observed that the improvement percentage increased by the value of the Nusselt number when increasing the amplitude of the wave, in order to increase the surface area as well as the turbulence generated within the flow.

Key areas for future studies include expanding the analysis to turbulent flows using advanced turbulence modeling, investigating different working fluids and Prandtl numbers, analyzing additional waveforms and orientations, experimental validation focused on pulsating flows in wavy geometries, and applying the model to optimize real-world systems like fuel cells and electronics cooling. Further research should also explore effects across a wider range of parameters, alternative channel geometries, and more complex wave patterns.

Nomenclatures

Symbols	description
c_p	Specific heat at constant pressure [J/kg.K]
H	High of channel [m]
h	heat transfer coefficient [W/m ² .K]
k	Thermal conductivity [W/m. K]
Nu	Nusselt number
P	pressure [Pa]
Pr	Prandtl number.
q	Heat transfer rate [W]
Re	Reynolds number
St	Strouhal number
T	Inlet Temperature [K]
u, v	x-y velocity components [m/s]

Greek Symbols	
μ	Dynamic viscosity [Pa.s]
α	Wavy amplitude
θ	dimensionless temperature
ν	Kinematic viscosity of the fluid [m ² /s]
ρ	Density [kg/m ³]
τ	Dimensionless time
β	Wavy number
Subscripts	
a.t	Time Average
in	input

REFERENCES

- [1] H. Zontul, N. Kurtulmuş, and B. Şahin, "Pulsating flow and heat transfer in wavy channel with zero degree phase shift," *European Mechanical Science*, vol. 1, no. 1, pp. 31-38, 2017.
- [2] M. Jafari, M. Farhadi, and K. Sedighi, "Convection heat transfer of SWCNT-nanofluid in a corrugated channel under pulsating velocity profile," *International communications in heat and mass transfer*, vol. 67, pp. 137-146, 2015. <http://dx.doi.org/10.1016/j.icheatmasstransfer.2015.07.008>
- [3] T. K. Nandi and H. Chattopadhyay, "Numerical investigations of simultaneously developing flow in wavy microchannels under pulsating inlet flow condition," *International communications in heat and mass transfer*, vol. 47, pp. 27-31, 2013. <http://dx.doi.org/10.1016/j.icheatmasstransfer.2013.06.008>
- [4] U. Akdag, S. Akcay, and D. Demiral, "Heat transfer enhancement with nanofluids under laminar pulsating flow in a trapezoidal-corrugated channel," *Progress in Computational Fluid Dynamics, An International Journal*, vol. 17, no. 5, pp. 302-312, 2017. <https://doi.org/10.1504/PCFD.2017.086322>
- [5] C. Pang, J. W. Lee, and Y. T. Kang, "Review on combined heat and mass transfer characteristics in nanofluids," *International Journal of Thermal Sciences*, vol. 87, pp. 49-67, 2015. <http://dx.doi.org/10.1016/j.ijthermalsci.2014.07.017>
- [6] A. A. Al-Rashed, A. Shahsavari, S. Entezari, M. Moghimi, S. A. Adio, and T. K. Nguyen, "Numerical investigation of non-Newtonian water-CMC/CuO nanofluid flow in an offset strip-fin microchannel heat sink: thermal performance and thermodynamic considerations," *Applied Thermal Engineering*, vol. 155, pp. 247-258, 2019. <https://doi.org/10.1016/j.applthermaleng.2019.04.009>
- [7] J.-C. Yang, F.-C. Li, Y.-R. He, Y.-M. Huang, and B.-C. Jiang, "Experimental study on the characteristics of heat transfer and flow resistance in turbulent pipe flows of viscoelastic-fluid-based Cu nanofluid," *International Journal of Heat and Mass Transfer*, vol. 62, pp. 303-313, 2013. <http://dx.doi.org/10.1016/j.ijheatmasstransfer.2013.02.074>
- [8] J. Saien and R. Hasani, "Hydrodynamics and mass transfer characteristics of circulating single drops with effect of different size nanoparticles," *Separation and Purification Technology*, vol. 175, pp. 298-304, 2017. <http://dx.doi.org/10.1016/j.seppur.2016.11.043>
- [9] H. Heidary and M. Kermani, "Effect of nano-particles on forced convection in sinusoidal-wall channel," *International Communications in Heat and Mass Transfer*, vol. 37, no. 10, pp. 1520-1527, 2010. <http://dx.doi.org/10.1016/j.icheatmasstransfer.2010.08.018>
- [10] A. A. Minea and W. M. El-Maghlany, "Influence of hybrid nanofluids on the performance of parabolic trough collectors in solar thermal systems: recent findings and numerical

- comparison," *Renewable Energy*, vol. 120, pp. 350-364, 2018.<http://dx.doi.org/10.1016/j.renene.2017.12.093>.
- [11] P. Li, D. Zhang, Y. Xie, and G. Xie, "Flow structure and heat transfer of non-Newtonian fluids in microchannel heat sinks with dimples and protrusions," *Applied Thermal Engineering*, vol. 94, pp. 50-58, 2016.<http://dx.doi.org/10.1016/j.applthermaleng.2015.10.119>.
- [12] A. Ebrahimi, B. Naranjani, S. Milani, and F. D. Javan, "Laminar convective heat transfer of shear-thinning liquids in rectangular channels with longitudinal vortex generators," *Chemical Engineering Science*, vol. 173, pp. 264-274, 2017.<http://dx.doi.org/10.1016/j.ces.2017.07.044>.
- [13] E. Taheran and K. Javaherdeh, "Experimental investigation on the effect of inlet swirl generator on heat transfer and pressure drop of non-Newtonian nanofluid," *Applied Thermal Engineering*, vol. 147, pp. 551-561, 2019.<https://doi.org/10.1016/j.applthermaleng.2018.07.142>.
- [14] H. G. Langeroudi and K. Javaherdeh, "Experimental study of non-Newtonian fluid flow inside the corrugated tube inserted with typical and V-cut twisted tapes," *Heat and Mass Transfer*, vol. 55, no. 4, pp. 937-951, 2019.<https://doi.org/10.1007/s00231-018-2467-3>.
- [15] P. Li, Y. Xie, and D. Zhang, "Laminar flow and forced convective heat transfer of shear-thinning power-law fluids in dimpled and protruded microchannels," *International Journal of Heat and Mass Transfer*, vol. 99, pp. 372-382, 2016.<http://dx.doi.org/10.1016/j.ijheatmasstransfer.2016.04.04>.
- [16] D. Crespi-Llorens, P. Vicente, and A. Viedma, "Experimental study of heat transfer to non-Newtonian fluids inside a scraped surface heat exchanger using a generalization method," *International Journal of Heat and Mass Transfer*, vol. 118, pp. 75-87, 2018.<https://doi.org/10.1016/j.ijheatmasstransfer.2017.10.115>.
- [17] W. Duangthongsuk and S. Wongwises, "An experimental investigation of the heat transfer and pressure drop characteristics of a circular tube fitted with rotating turbine-type swirl generators," *Experimental thermal and fluid science*, vol. 45, pp. 8-15, 2013.<http://dx.doi.org/10.1016/j.expthermflsci.2012.09.009>.
- [18] Z. Ismail and R. Karim, "Laminar flow heat transfer of dilute viscoelastic solutions in flattened tube heat exchangers," *Applied thermal engineering*, vol. 39, pp. 171-178, 2012.<http://dx.doi.org/10.1016/j.applthermaleng.2012.01.046>.
- [19] A. M. Jawarneh, M. Al-Widyan, and Z. Al-Mashhadani, "Experimental study on heat transfer augmentation in a double pipe heat exchanger utilizing jet vortex flow," *Heat Transfer*, vol. 52, no. 1, pp. 317-332, 2023.<https://doi.org/10.1002/htj.22696>.
- [20] A. M. Jawarneh, "Heat transfer enhancement in a narrow concentric annulus in decaying swirl flow," *Heat transfer research*, vol. 42, no. 3, pp. 2011.<https://doi.org/10.1615/HeatTransRes.2011001197>.
- [21] H. Zhang, S. Li, J. Cheng, Z. Zheng, X. Li, and F. Li, "Numerical study on the pulsating effect on heat transfer performance of pseudo-plastic fluid flow in a manifold microchannel heat sink," *Applied Thermal Engineering*, vol. 129, pp. 1092-1105, 2018.<https://doi.org/10.1016/j.applthermaleng.2017.10.124>.
- [22] I. Elbadawy, A. Sabry, M. H. Shedid, and A. Basheer, "Heat transfer characteristics in wake region of a single finned obstacle," *International Journal of Thermal Sciences*, vol. 128, pp. 149-159, 2018.<https://doi.org/10.1016/j.ijthermalsci.2018.01.017>.
- [23] A. A. Alkhafaji, A. A. Alkhalidi, and R. S. Amano, "Effect of Water Column Height on the Aeration Efficiency Using Pulsating Air Flow," *Jordan Journal of Mechanical and Industrial Engineering*, vol. 12, no. 1, 2018.
- [24] X.-Y. Tang, G. Jiang, and G. Cao, "Parameters study and analysis of turbulent flow and heat transfer enhancement in narrow channel with discrete grooved structures," *Chemical Engineering Research and Design*, vol. 93, pp. 232-250, 2015.<http://dx.doi.org/10.1016/j.cherd.2014.07.009>.
- [25] R. Kumar, R. Chauhan, M. Sethi, A. Sharma, and A. Kumar, "Experimental investigation of effect of flow attack angle on thermohydraulic performance of air flow in a rectangular channel with discrete V-pattern baffle on the heated plate," *Advances in Mechanical Engineering*, vol. 8, no. 5, p. 1687814016641056, 2016.<http://dx.doi.org/10.1177/1687814016641056>.
- [26] R. Ali and A. Singh, "Numerical Study of Fluid Dynamics and Heat Transfer Characteristics for the Flow Past a Heated Square Cylinder," *Jordan Journal of Mechanical and Industrial Engineering*, vol. 15, no. 4, 2021.
- [27] J. Ganesh Murali and S. S. Katte, "Experimental investigation of heat transfer enhancement in radiating pin fin," *Jordan Journal of Mechanical and Industrial Engineering*, vol. 2, pp. 163-167, 2008.
- [28] P. Murugesan, K. Mayilsamy, and S. Sures, "Heat transfer and friction factor in a tube equipped with U-cut twisted tape insert," *JJMIE*, vol. 5, no. 6, pp. 559-565, 2011.
- [29] A. S. Yadav, "Effect of half length twisted-tape turbulators on heat transfer and pressure drop characteristics inside a double pipe u-bend heat exchanger," *JJMIE*, vol. 3, no. 1, pp. 17-22, 2009.
- [30] M.-A. Moon, M.-J. Park, and K.-Y. Kim, "Evaluation of heat transfer performances of various rib shapes," *International Journal of Heat and Mass Transfer*, vol. 71, pp. 275-284, 2014.<http://dx.doi.org/10.1016/j.ijheatmasstransfer.2013.12.026>.
- [31] O. Oyewola, O. Ismail, and K. Abu, "Numerical Simulation of Forced Convection Flows over a Pair of Circular Cylinders in Tandem Arrangement," *Jordan Journal of Mechanical and Industrial Engineering*, vol. 13, no. 4, 2019.
- [32] N. Mikheev, V. Molochnikov, I. Davletshin, and O. Dushina, "Simulation of pulsating channel flows," *Russian Aeronautics (Iz VUZ)*, vol. 52, no. 1, pp. 77-82, 2009.
- [33] A. Goltsman, I. Davletshin, N. Mikheev, and A. Paereliy, "Shear stresses in turbulent pulsating channel flow," *Thermophysics and Aeromechanics*, vol. 22, no. 3, pp. 319-328, 2015.
- [34] I. Zahmatkesh and S. A. Naghedifar, "Pulsating Nanofluid Jet Impingement onto a Partially Heated Surface Immersed in a Porous Layer," *Jordan Journal of Mechanical and Industrial Engineering*, vol. 12, no. 2, 2018.
- [35] P. Papadopoulos and A. Vouros, "Pulsating turbulent pipe flow in the current dominated regime at high and very-high frequencies," *International Journal of Heat and Fluid Flow*, vol. 58, pp. 54-67, 2016.<http://dx.doi.org/10.1016/j.ijheatfluidflow.2015.12.007>.
- [36] A. Witte and W. Polifke, "Dynamics of unsteady heat transfer in pulsating flow across a cylinder," *International Journal of Heat and Mass Transfer*, vol. 109, pp. 1111-1131, 2017.<http://dx.doi.org/10.1016/j.ijheatmasstransfer.2017.02.072>.
- [37] H. Yuan, S. Tan, J. Wen, and N. Zhuang, "Heat transfer of pulsating laminar flow in pipes with wall thermal inertia," *International Journal of Thermal Sciences*, vol. 99, pp. 152-160, 2016.<http://dx.doi.org/10.1016/j.ijthermalsci.2015.08.014>.
- [38] R. Hossain, M. Chowdhuri, and C. Feroz, "Design, Fabrication and Experimental Study of Heat Transfer Characteristics of a Micro Heat Pipe," *Jordan Journal of Mechanical and Industrial Engineering*, vol. 4, no. 5, 2010.

- [39] M. Saraireh, "Computational fluid dynamics simulation of plate fin and circular pin fin heat sinks," *Jordan Journal of Mechanical and Industrial Engineering*, vol. 10, no. 2, pp. 99-104, 2016.
- [40] A. A. Mehri, M. Farhadi, and S. Shayamehr, "Natural convection flow of Cu-Water nanofluid in horizontal cylindrical annuli with inner triangular cylinder using lattice Boltzmann method," *International Communications in Heat and Mass Transfer*, vol. 44, pp. 147-156, 2013. <http://dx.doi.org/10.1016/j.icheatmasstransfer.2013.03.001>
- [41] A. Naddaf, S. Z. Heris, and B. Pouladi, "An experimental study on heat transfer performance and pressure drop of nanofluids using graphene and multi-walled carbon nanotubes based on diesel oil," *Powder Technology*, vol. 352, pp. 369-380, 2019. <https://doi.org/10.1016/j.powtec.2019.04.078>.
- [42] B. R. Ponangi, S. Sumanth, V. Krishna, T. Seetharam, and K. Seetharamu, "Heat transfer analysis of radiator using graphene oxide nanofluids," in *IOP Conference Series: Materials Science and Engineering*, 2018, vol. 346, no. 1: IOP Publishing, p. 012032. <https://doi.org/10.1016/10.1088/1757-899X/346/1/012032>.
- [43] R. Ranjbarzadeh, A. M. Isfahani, M. Afrand, A. Karimipour, and M. Hojjati, "An experimental study on heat transfer and pressure drop of water/graphene oxide nanofluid in a copper tube under air cross-flow: applicable as a heat exchanger," *Applied Thermal Engineering*, vol. 125, pp. 69-79, 2017. <http://dx.doi.org/10.1016/j.applthermaleng.2017.06.110>
- [44] M. R. Esfahani, E. M. Languri, and M. R. Nunna, "Effect of particle size and viscosity on thermal conductivity enhancement of graphene oxide nanofluid," *International Communications in Heat and Mass Transfer*, vol. 76, pp. 308-315, 2016. <http://dx.doi.org/10.1016/j.icheatmasstransfer.2016.06.006>.
- [45] M. Sajjad, M. S. Kamran, R. Shaukat, and M. I. M. Zeinelabdeen, "Numerical investigation of laminar convective heat transfer of graphene oxide/ethylene glycol-water nanofluids in a horizontal tube," *Engineering science and technology, an international journal*, vol. 21, no. 4, pp. 727-735, 2018. <https://doi.org/10.1016/j.jestch.2018.06.009>.
- [46] D. Jin, Y. Lee, and D.-Y. Lee, "Effects of the pulsating flow agitation on the heat transfer in a triangular grooved channel," *International journal of heat and mass transfer*, vol. 50, no. 15-16, pp. 3062-3071, 2007. <https://doi.org/10.1016/j.ijheatmasstransfer.2006.12.001>
- [47] U. Akdag, S. Akcay, and D. Demiral, "Heat transfer enhancement with laminar pulsating nanofluid flow in a wavy channel," *International Communications in Heat and Mass Transfer*, vol. 59, pp. 17-23, 2014. <http://dx.doi.org/10.1016/j.icheatmasstransfer.2014.10.008>.
- [48] R. Bouakkaz, Y. Khelili, and F. Salhi, "Unconfined laminar nanofluid flow and heat transfer around a square cylinder with an angle of incidence," *Jordan Journal of Mechanical and Industrial Engineering*, vol. 13, no. 3, pp. 191-196, 2019.
- [49] A. Japper-Jaafar, M. Escudier, and R. Poole, "Laminar, transitional and turbulent annular flow of drag-reducing polymer solutions," *Journal of Non-Newtonian Fluid Mechanics*, vol. 165, no. 19-20, pp. 1357-1372, 2010. <http://dx.doi.org/10.1016/j.jnnfm.2010.07.001>.
- [50] L. Broniarz-Press and K. Pralat, "Thermal conductivity of Newtonian and non-Newtonian liquids," *International journal of heat and mass transfer*, vol. 52, no. 21-22, pp. 4701-4710, 2009. <http://dx.doi.org/10.1016/j.ijheatmasstransfer.2009.06.019>
- [51] H. Inaba, W. I. Aly, N. Haruki, and A. Horibe, "Flow and heat transfer characteristics of drag reducing surfactant solution in a helically coiled pipe," *Heat and mass transfer*, vol. 41, no. 10, pp. 940-952, 2005. <http://dx.doi.org/10.1007/s00231-004-0599-0>.
- [52] J. Zhang, J. Kundu, and R. M. Manglik, "Effect of fin waviness and spacing on the lateral vortex structure and laminar heat transfer in wavy-plate-fin cores," *International Journal of Heat and Mass Transfer*, vol. 47, no. 8-9, pp. 1719-1730, 2004. <http://dx.doi.org/10.1016/j.ijheatmasstransfer.2003.10.006>.
- [53] Y. Sui, C. Teo, and P. Lee, "Direct numerical simulation of fluid flow and heat transfer in periodic wavy channels with rectangular cross-sections," *International Journal of Heat and Mass Transfer*, vol. 55, no. 1-3, pp. 73-88, 2012. <http://dx.doi.org/10.1016/j.ijheatmasstransfer.2011.08.041>.
- [54] X. W. Zhu, Y. H. Fu, J. Q. Zhao, and L. Zhu, "Three-dimensional numerical study of the laminar flow and heat transfer in a wavy-finned heat sink filled with Al₂O₃/ethylene glycol-water nanofluid," *Numerical Heat Transfer, Part A: Applications*, vol. 69, no. 2, pp. 195-208, 2016. <http://dx.doi.org/10.1080/10407782.2015.1052323>.
- [55] R. Kalaivanan and R. Rathnasamy, "Experimental investigation of forced convective heat transfer in rectangular micro-channels," *Jordan Journal of Mechanical and Industrial Engineering*, vol. 5, no. 5, p. 383, 2011.
- [56] H. Laidoudi et al., "Numerical Investigation of Buoyancy-driven Flow in a Crescent-shaped Enclosure," *Jordan Journal of Mechanical and Industrial Engineering*, vol. 16, no. 4, 2022.
- [57] A. M. Hassan, A. A. Alwan, and H. K. Hamzah, "Metallic foam with cross flow heat exchanger: A review of parameters, performance, and challenges," *Heat Transfer*, vol. 52, no. 3, pp. 2618-2650, 2023. <https://doi.org/10.1002/htj.22798>
- [58] R. M. K. Ali and S. L. Ghashim, "Thermal performance analysis of heat transfer in pipe by using metal foam," *Jordan Journal of Mechanical and Industrial Engineering*, vol. 17, no. 2, 2023.
- [59] B. Zhong and W. Li, "Modeling and Analysis of Relationship Between Flow Characteristics and Efficiency of Reciprocating Porous Medium Burner," *Jordan Journal of Mechanical and Industrial Engineering (JJMIE)*, vol. 16, no. 1, 2022.
- [60] A. M. Hassan, A. A. Alwan, and H. K. Hamzah, "Experimental study of thermal performance improvement in a cross-flow heat exchanger by using copper foam," *Heat Transfer*, vol. 52, no. 6, pp. 4078-4108, 2023. <https://doi.org/10.1002/htj.22867>
- [61] S. Shawish, D. B. Mostafa, R. Al-Waked, and M. S. Nasif, "CFD Simulation of Energy Transfer within a Membrane Heat Exchanger under Turbulent Flow," *Jordan Journal of Mechanical and Industrial Engineering JJMIE*, vol. 17, no. 2, 2023.
- [62] Z. K. Kadim and K. A. Khalaf, "Numerical study of heat transfer enhancement in contour corrugated channel using water and engine oil," *CFD Letters*, vol. 12, no. 12, pp. 17-37, 2020. <https://doi.org/10.37934/cfdl.12.12.1737>
- [63] J. Galindo, P. Fajardo, R. Navarro, and L. García-Cuevas, "Characterization of a radial turbocharger turbine in pulsating flow by means of CFD and its application to engine modeling," *Applied Energy*, vol. 103, pp. 116-127, 2013. <http://dx.doi.org/10.1016/j.apenergy.2012.09.013>
- [64] S. Marelli and M. Capobianco, "Steady and pulsating flow efficiency of a waste-gated turbocharger radial flow turbine for automotive application," *Energy*, vol. 36, no. 1, pp. 459-465, 2011. <http://dx.doi.org/10.1016/j.energy.2010.10.019>.